

[2]Pseudorotaxanes from T-Shaped Benzimidazolium Axles and [24]Crown-8 Wheels

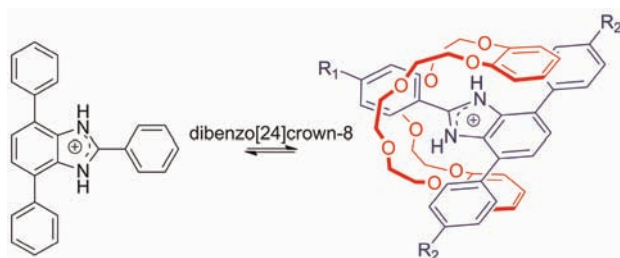
Nadim Noujeim, Kelong Zhu, V. Nicholas Vukotic, and Stephen J. Loeb*

Department of Chemistry and Biochemistry, University of Windsor, Windsor, Ontario N9B 3P4, Canada

loeb@uwindsor.ca

Received March 24, 2012

ABSTRACT



A new templating motif for the formation of [2]pseudorotaxanes is described in which T-shaped axles with a benzimidazolium core and aromatic substituents at the 2-, 4-, and 7-positions interact with [24]crown-8 ether wheels ([24]crown-8, dibenzo[24]crown-8, and dinaphtho[24]crown-8). The T-shape greatly enhances the association between axle and wheel when compared to simple imidazolium or benzimidazolium cations. A series of interpenetrated molecules are characterized by ^1H NMR spectroscopy and single crystal X-ray crystallography.

[2]Pseudorotaxanes formed between electron-rich macrocyclic wheels and charged, electron-poor axles are often essential precursors for the synthesis of [2]rotaxanes via the threading-followed-by-stoppering protocol.^{1,2} Indeed, discovering new templating pairs of axles and wheels for [2]pseudorotaxane formation and investigating the fundamental nature of their interactions is vital for the development

of new mechanically interlocked molecules (MIMs) and their applications as molecular switches and machinery.^{3,4}

In our search for new axles to create [2]rotaxane ligands for applications in condensed materials,^{5,6} we were intrigued by the 2,4,7-substitution pattern of the benzimidazolium ion because this arrangement provides a rare example of an organic molecule with a rigid core and right angle (90°) turn. Unfortunately, the interaction of dibenzo[24]crown-8 (**DB24C8**) with either the imidazolium ($K_a = 8 \text{ M}^{-1}$)⁷ or phenylbenzimidazolium⁸ ($K_a = 54 \text{ M}^{-1}$) cation is quite weak. Tiburcio⁹ and Clarkson¹⁰ have reported

(1) (a) Huang, F.; Gibson, H. W. *Prog. Polym. Sci.* **2005**, *30*, 982. (b) Suzuki, S.; Nakazono, K.; Takata, T. *Org. Lett.* **2010**, *12*, 712. (c) Makita, Y.; Kihara, N.; Takata, T. *J. Org. Chem.* **2008**, *73*, 9245. (d) Makita, Y.; Kihara, N.; Takata, T. *Chem. Lett.* **2007**, *36*, 102. (e) Kawasaki, H.; Kihara, N.; Takata, T. *Chem. Lett.* **1999**, 1015. (f) Ko, J.-L.; Ueng, S.-H.; Chiu, C.-W.; Lai, C.-C.; Liu, Y.-H.; Peng, S.-M.; Chiu, S.-H. *Chem.—Eur. J.* **2010**, *16*, 6950. (g) Li, S.; Liu, M.; Zhang, J.; Zheng, B.; Zhang, C.; Wen, X.; Li, N.; Huang, F. *Org. Biomol. Chem.* **2008**, *6*, 2103. (h) Braunschweig, A. B.; Dichtel, W. R.; Miljanic, O. S.; Olson, M. A.; Spruell, J. M.; Khan, S. I.; Heath, J. R.; Stoddart, J. F. *Chem. Asian J.* **2007**, *2*, 634. (i) Braunschweig, A. B.; Ronconi, C. M.; Han, J.-Y.; Arico, F.; Cantrill, S. J.; Stoddart, J. F.; Khan, S. I.; White, A. J. P.; Williams, D. J. *Eur. J. Org. Chem.* **2006**, 1857. (j) Rowan, S. J.; Cantrill, S. J.; Stoddart, J. F. *Org. Lett.* **1999**, *1*, 129.

(2) Loeb, S. J.; Wisner, J. A. *Angew. Chem., Int. Ed.* **1998**, *37*, 2838. (3) (a) Balzani, V.; Credi, A.; Venturi, M. *Molecular Devices and Machines – Concepts and Perspectives for the Nanoworld*; Wiley-Interscience, Wiley-VCH: Weinheim, 2008. (b) Kay, E. K.; Leigh, D. A.; Zerbetto, F. *Angew. Chem., Int. Ed.* **2007**, *46*, 72. (c) Coskun, A.; Banaszak, M.; Astumian, R. D.; Stoddart, J. F.; Grzybowski, B. A. *Chem. Soc. Rev.* **2012**, *41*, 19.

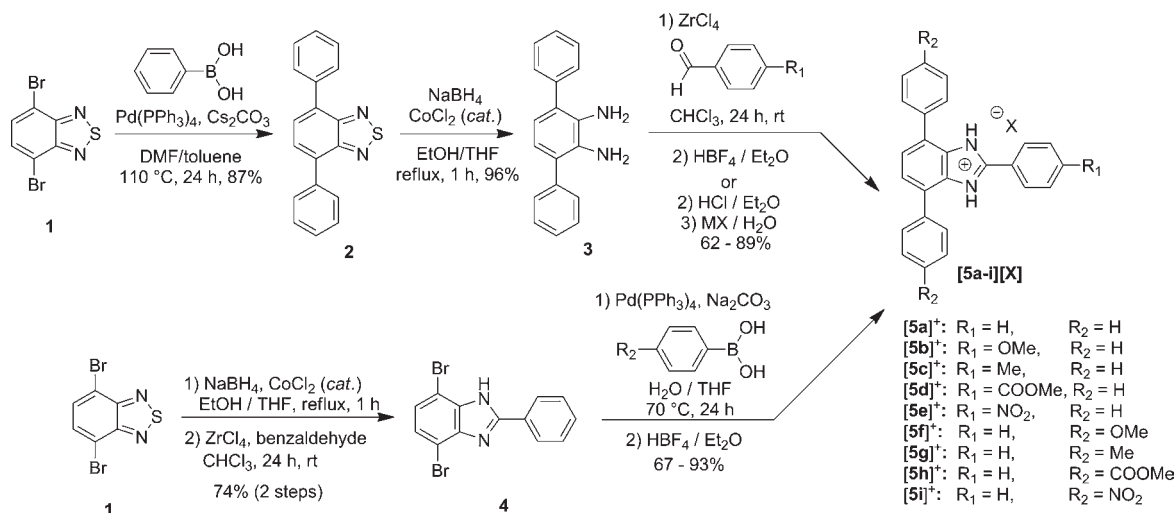
(4) (a) Davidson, G. J. E.; Sharma, S.; Loeb, S. J. *Angew. Chem., Int. Ed.* **2010**, *49*, 4938. (b) Loeb, S. J.; Tiburcio, J.; Vella, S. J. *Chem. Commun* **2006**, 1598. (c) Suhan, N. D.; Allen, L.; Gharib, M. T.; Viljoen, E.; Vella, S. J.; Loeb, S. J. *Chem. Commun.* **2011**, *47*, 5991.

(5) Loeb, S. J. *Rotaxanes as Ligands: From Molecules to Materials in Organic Nanostructures InterScience*; Steed, J. W., Atwood, J. L., Eds.; Wiley-VCH: Weinheim, 2008; p 33.

(6) (a) Loeb, S. J. *Chem. Soc. Rev.* **2007**, *36*, 226. (b) Davidson, G. J. E.; Loeb, S. J. *Angew. Chem., Int. Ed.* **2003**, *42*, 74. (c) Hoffart, D. J.; Loeb, S. J. *Angew. Chem., Int. Ed.* **2005**, *44*, 901. (d) Hoffart, D. J.; Loeb, S. J. *Supramol. Chem.* **2007**, *19*, 89. (e) Knight, L. K.; Vukotic, V. N.; Viljoen, E.; Caputo, C. B.; Loeb, S. J. *Chem. Commun.* **2009**, 5585. (f) Vukotic, V. N.; Loeb, S. J. *Chem.—Eur. J.* **2010**, *16*, 13630. (g) Mercer, D. J.; Vukotic, V. N.; Loeb, S. J. *Chem. Commun.* **2011**, *47*, 896.

(7) Kiviniemi, S.; Nissinen, M.; Jorma-Jalonen, M. T.; Rissanen, K.; Lämsä, M.; Pursiainen, J. *New J. Chem.* **2000**, *24*, 47.

Scheme 1. Synthesis of 2,4,7-Triphenylbenzimidazolium Axles^{a,b}



^a See the Supporting Information for details.

^b For **5a**: MX = NH₄BF₄, NH₄PF₆, NH₄OTf, LiClO₄ or LiNTf₂. For **5b**–**i**: MX = NH₄BF₄ only.

that, similar to 1,2-bis(pyridinium)ethane axles,^{2,11,12} when benzimidazolium groups are linked by a two-carbon chain, the association constant can be effectively increased, but this type of flexible axle was not suitable for our purposes and is not easily functionalized.¹³

As a preliminary test, we prepared the T-shaped 2,4,7-triphenylbenzimidazolium cation as the BF₄ salt (Scheme 1) and measured the association constant for [2]pseudorotaxane formation with **DB24C8**. The ¹H NMR spectrum of a CD₃CN solution comprising equimolar amounts of [5a]⁺ and **DB24C8** (1.0 × 10⁻³ M, 298 K) showed efficient formation of [2]pseudorotaxane [5a⊂DB24C8]⁺. Surprisingly, the resulting association constant (1.78 × 10³ M⁻¹) was orders of magnitude larger than those found for simple imidazolium or benzimidazolium derivatives.^{7,8}

Based on the efficient [2]pseudorotaxane formation observed for [5a⊂DB24C8]⁺, we undertook a detailed study of this new templating motif to (1) pinpoint the source of the dramatic increase in association relative to simple imidazolium cations and (2) determine the breadth and tunability of the interaction. Three 24-membered

Table 1. Effect of Solvent and Counterion on Association Constant for [2]Pseudorotaxane [5a⊂DB24C8]⁺^a

counterion ^b	solvent	K _{assoc} ^c (M ⁻¹)
PF ₆	CD ₃ CN	1290
OTf	CD ₃ CN	300
NTf ₂	CD ₃ CN	370
ClO ₄	CD ₃ CN	390
BF ₄	CD ₃ CN	1780
BF ₄	CD ₃ OD	90
BF ₄	(CD ₃) ₂ CO	400
BF ₄	CD ₃ NO ₂	3900
BF ₄	CD ₂ Cl ₂	75200

^a ¹H NMR spectroscopy (1.0 × 10⁻³ M, 298 K). ^b OTf = CF₃SO₃, NTf₂ = N(CF₃SO₂)₂. ^c Errors are estimated to be less than 10%.

Table 2. Effect of Axle Substituents on Association Constants^a

axle	R ₁	R ₂	K _{assoc} ^b (M ⁻¹)		
			DN24C8	24C8	DB24C8
[5a] ⁺	H	H	1300	1670	1780
[5b] ⁺	OMe	H	820	1170	760
[5c] ⁺	Me	H	880	1180	850
[5d] ⁺	COOMe	H	3840	3720	4410
[5e] ⁺	NO ₂	H	6180	5970	6930
[5f] ⁺	H	OMe	1880	1350	1120
[5g] ⁺	H	Me	1520	1030	890
[5h] ⁺	H	COOMe	2810	1710	2580
[5i] ⁺	H	NO ₂	2900	2430	3520

^a ¹H NMR spectroscopy (CD₃CN, 1.0 × 10⁻³ M, 298 K). ^b Errors are estimated to be less than 10%.

(8) Zhu, K.; Vukotic, V. N.; Loeb, S. J. *Angew. Chem., Int. Ed.* **2012**, *51*, 2168.

(9) Castillo, D.; Astudillo, P.; Mares, J.; González, F. J.; Vela, A.; Tiburcio, J. *Org. Biomol. Chem.* **2007**, *5*, 2252.

(10) Li, L.; Clarkson, G. J. *Org. Lett.* **2007**, *9*, 497.

(11) (a) Mercer, D. J.; Vella, S. J.; Guertin, L.; Suhan, N. D.; Tiburcio, J.; Vukotic, V. N.; Wisner, J. A.; Loeb, S. J. *Eur. J. Org. Chem.* **2011**, 1763. (b) Loeb, S. J.; Tiburcio, J.; Vella, S. J.; Wisner, J. A. *Org. Biomol. Chem.* **2006**, *4*, 667.

(12) (a) Loeb, S. J.; Tiburcio, J.; Vella, S. J. *Org. Lett.* **2005**, *7*, 4923. (b) Georges, N.; Loeb, S. J.; Tiburcio, J.; Wisner, J. A. *Org. Biomol. Chem.* **2004**, *2*, 2751. (c) Vella, S. J.; Tiburcio, J.; Gauld, J. W.; Loeb, S. J. *Org. Lett.* **2006**, *8*, 3421. (d) Sharma, S.; Davidson, G. J. E.; Loeb, S. J. *Chem. Commun.* **2008**, 582.

(13) (a) Noujeim, N.; Leclercq, L.; Schmitzer, A. R. *J. Org. Chem.* **2008**, *73*, 3784. (b) Mukhopadhyay, C.; Ghosh, S.; Schmiedekamp, A. M. *Org. Biomol. Chem.* **2012**, *10*, 1434.

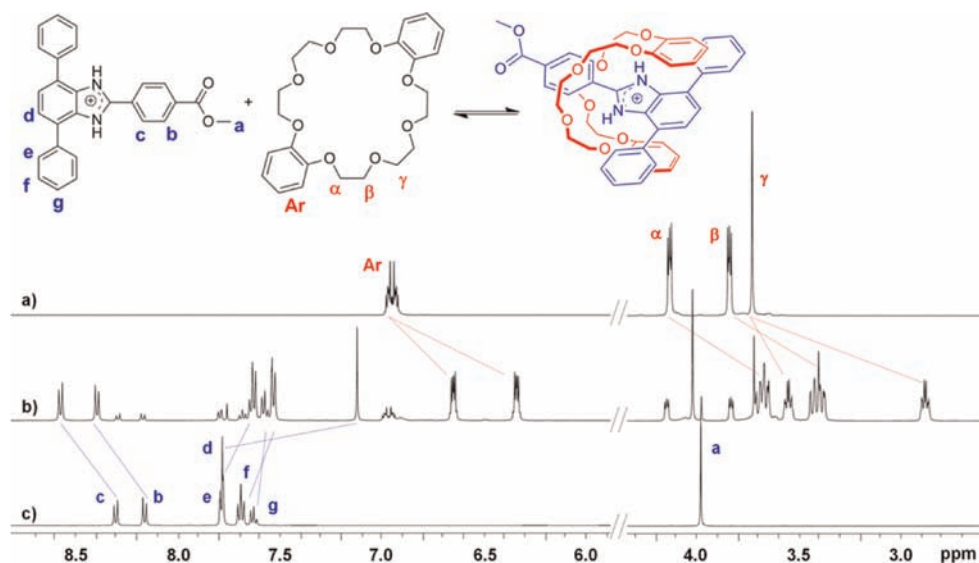


Figure 1. ^1H NMR spectra (298 K, CD_3CN , 1.0×10^{-2} M) of (a) wheel **DB24C8**; (b) an equimolar solution of $[\mathbf{5d}][\text{BF}_4]$ and **DB24C8** showing formation of $[\mathbf{2}]$ pseudorotaxane $[\mathbf{5d} \subset \text{DB24C8}][\text{BF}_4]$; (c) axle $[\mathbf{5d}][\text{BF}_4]$.

crown ether wheels, **24C8** ([24]crown-8), **DB24C8**, and **DN24C8** (dinaphtho[24]crown-8), were combined with benzimidazolium axles containing various electron-donating (EDG) and withdrawing groups (EWG) as substituents (R_1 and R_2) on the three aromatic rings.

The 2,4,7-triphenylbenzimidazolium cations ($[\mathbf{5a}]^+ - [\mathbf{5i}]^+$) were prepared in good yields as outlined in Scheme 1. Only those axles with either R_1 or $\text{R}_2 = \text{H}$ were studied to simplify the analysis of EDG and EWG contributions. As outlined in Scheme 1, two synthetic routes were employed; (1) R_1 groups were introduced using a condensation/oxidation step¹⁴ from the diamine **3** where $\text{R}_2 = \text{H}$ and (2) R_2 groups were introduced via Suzuki coupling using the 4,7-dibromobenzimidazole **4** where $\text{R}_1 = \text{H}$.

Association constants were determined by ^1H NMR spectroscopy and are summarized in Tables 1 and 2. Exchange between complexed and uncomplexed species was slow on the NMR time scale for all samples. In each case, significant shifts to higher frequency were observed for the NH and *c* resonances on the axle indicative of hydrogen-bonding between axle and wheel. Shifts to lower frequency for aromatic proton *d* on the axle and Ar protons on the wheel also occur with **DB24C8** or **DN24C8** due to efficient π -stacking between the electron poor benzimidazolium ring and the electron-rich catechol rings of the crown ether (Figure 1).

Initially, the salts $[\mathbf{5a}][\text{X}]$ ($\text{X} = \text{PF}_6, \text{CF}_3\text{SO}_3, \text{N}(\text{CF}_3\text{SO}_2)_2, \text{ClO}_4, \text{and BF}_4$) were studied with **DB24C8** in CD_3CN . It was observed that the BF_4 salts yielded the

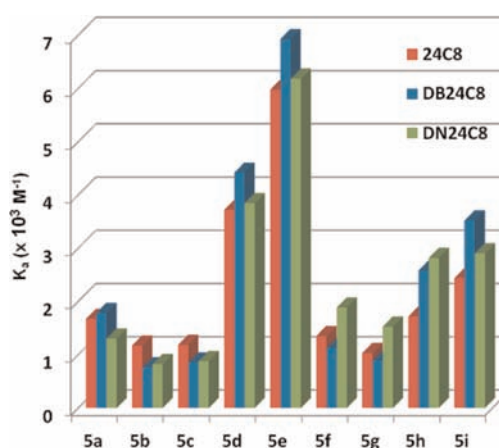


Figure 2. Plot illustrating the variation in association constant for $[\mathbf{2}]$ pseudorotaxane formation as a function of axle substituents and crown ether wheel.

largest association constants under these conditions (Table 1).¹⁵ The effect of solvent on the formation of $[\mathbf{5a} \subset \text{DB24C8}]^+$ was shown to be $\text{CD}_3\text{OD} < (\text{CD}_3)_2\text{CO} < \text{CD}_3\text{CN} < \text{CD}_3\text{NO}_2 < \text{CD}_2\text{Cl}_2$ (Table 1).¹⁶ The combination of $\text{X} = \text{BF}_4$ and CD_3CN was chosen for the detailed study involving variation of the axle substituents in order to allow for a large range in association constants and ensure the solubility of all the components. Association constants for $[\mathbf{2}]$ pseudorotaxane formation

(14) Akpınar, H.; Balan, A.; Baran, D.; Unver, E.; Toppare, L. *Polymer* **2010**, *51*, 6123.

(15) Gibson, H. W.; Jones, J. W.; Zakharov, L. N.; Rheingold, A. L.; Sledobnick, C. *Chem.—Eur. J.* **2011**, *17*, 3192. (b) Zhu, K.; Li, S.; Wang, F.; Huang, F. *J. Org. Chem.* **2009**, *74*, 1322. (c) Jones, J. W.; Gibson, H. W. *J. Am. Chem. Soc.* **2003**, *125*, 7001.

(16) (a) Horn, J. R.; Russell, D.; Lewis, E. A.; Murphy, K. P. *Biochemistry* **2001**, *40*, 1774. (b) Horn, J. R.; Brandts, J. F.; Murphy, K. P. *Biochemistry* **2002**, *41*, 7501. (c) Smithrud, D. B.; Wyman, T. B.; Diederich, F. *J. Am. Chem. Soc.* **1991**, *113*, 5420. (d) Stauffer, D. A.; Barrans, R. E., Jr.; Dougherty, D. A. *J. Org. Chem.* **1990**, *55*, 2762.

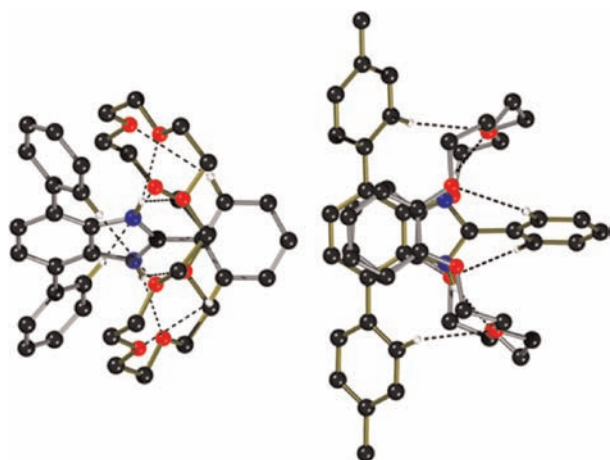


Figure 3. Ball-and-stick representations of the cationic portions of the single-crystal X-ray structures of $[5aCDB24C8][BF_4]$ (left) and $[5gCDB24C8][BF_4]$ (right). H-atoms not involved in hydrogen bonding have been omitted for clarity.

between **24C8**, **DB24C8**, and **DN234C8** and nine axles ($[5a]^+ - [5i]^+$) containing R_1 or $R_2 = H, OMe, Me, COOMe, NO_2$ were measured (Table 2).

When either R_1 or R_2 is an EWG, the hydrogen-bonding, ion-dipole, and π -stacking interactions are all strengthened due to an increase in acidity of hydrogen-bond donors and an increase in charge on the benzimidazolium rings; the presence of an EDG lowers the association constant by weakening these same interactions.^{12a} The effect is more pronounced for R_1 because substitution at the 2-position results in a more direct effect on the imidazolium moiety. A Van't Hoff plot $[5aCDB24C8]^+$ (see the Supporting Information) shows that the interaction between axle and wheel is driven primarily by enthalpic gain.¹⁶ Hammett plots for variations in R_1 with each crown ether are linear, supporting the straightforward effect of the added EDG/EWG substituents on hydrogen-bonding (see the Supporting Information).¹⁷ Figure 2 shows the variations in association constant with different axles and wheels in graphical format. In general, the addition of a larger aromatic ring system (changing from **DB24C8** to **DN24C8**) does not enhance binding due to increased steric interactions with the R_2 -substituted rings at the 4- and 7-positions of the benzimidazolium ring.

The X-ray structure¹⁸ of $[5aCDB24C8]^+$ (Figure 3, left) represents the simplest of axle ($R_1 = R_2 = H$) and wheel

(17) Hansch, C.; Leo, A.; Taft, R. W. *Chem. Rev.* **1991**, *91*, 165.

(18) Crystallographic data for the two structures reported in this communication have been deposited with the Cambridge Crystallographic Data Centre as supplementary publication nos. CCDC-872986 and -872987. Copies of the data can be obtained free of charge on application to CCDC at email: deposit@ccdc.cam.ac.uk.

(**24C8**) pairing. There are three pairs of hydrogen-bonding interactions between axle and wheel; $NH \cdots O$ (bifurcated 2.85 Å, 143°; 3.04 Å, 138°; bifurcated 2.93 Å, 138°; 3.03 Å, 143°), $CH_c \cdots O$ (bifurcated 3.44 Å, 137°; 3.69 Å, 147°; bifurcated 3.33 Å, 130°; 3.64 Å, 149°), and $CH_e \cdots O$ (3.89 Å, 173°; 3.83 Å, 171°). This hydrogen-bonding array is accompanied by significant ion-dipole interactions between the cationic charge on the benzimidazolium ring and the crown ether oxygen atoms. The extra stability afforded by the 2,4,7-substitution pattern appears to come from the extra $CH \cdots O$ hydrogen-bonding provided by the added aromatic rings; this is consistent with shifts observed for these protons (*c* and *e*) in solution by ¹H NMR spectroscopy. The rigidity of the axles also probably contributes to an increase in association constant by limiting entropic effects.

The X-ray structure¹⁸ of $[5gCDB24C8]^+$ (Figure 3, right) was also determined and the hydrogen-bonding interactions are very similar to those observed for $[5gCDB24C8]^+$; $NH \cdots O$ (2.84 Å, 160°; 2.86 Å, 160°), $CH_c \cdots O$ (3.81 Å, 160°; 3.54 Å, 151°) and $CH_e \cdots O$ (3.63 Å, 152°; 3.55 Å, 153°). The C-shape conformation adopted by the **DB24C8** macrocycle allows for the addition of π -stacking interactions by clamping around the electron poor benzimidazolium ring (3.64–4.76 Å).

The major advantages of this new templating motif reported herein are (1) a much stronger association between axle and crown ether wheel due to the T-shape of the benzimidazolium cation, (2) a modular synthesis which allows for the incorporation of a wide variety of functionalized aromatics onto the molecular scaffold utilizing commercially available materials with well established coupling methodologies, and (3) the potential to easily incorporate this new template into MIMs by incorporating the appropriate functional group at R_1 , for example, aldehyde for further condensation⁸ or olefin for metathesis.

Acknowledgment. This research work was supported by a NSERC of Canada Discovery grant to S.J.L. N.N. is grateful to the FQRNT (Quebec) for the awarding of a postdoctoral fellowship. V.N.V. is grateful to NSERC of Canada for the awarding of an Alexander Graham Bell Graduate Doctoral Scholarship and to the ICDD for a Ludo Frevel Crystallography Scholarship.

Supporting Information Available. Synthetic experimental details, NMR spectra, details of association constant measurements, Van't Hoff plot, Hammett plots, and X-ray structures (CIF). This material is available free of charge via the Internet at <http://pubs.acs.org>.

The authors declare no competing financial interest.